AD_____

Award Number: DAMD17-02-1-0119

TITLE: Sodium Iodide Symporter Gene Transfer for Imaging and Ablation of Prostate Cancer

PRINCIPAL INVESTIGATOR: Sissy M. Jhiang, Ph.D.

CONTRACTING ORGANIZATION: The Ohio State University Research Foundation
Columbus, Ohio 43210-1063

REPORT DATE: January 2003

TYPE OF REPORT: Annual

PREPARED FOR: U.S. Army Medical Research and Materiel Command
Fort Detrick, Maryland 21702-5012

REPORT DOCUMENTATION PAGE

Form Approved
OMB No. 074-0188

1. AGENCY USE ONLY (Leave blank)	2. REPORT DATE	3. REPORT TYPE AND DATES COVERED
	January 2003	Annual (15 Dec 01 - 14 Dec 02)

4. TITLE AND SUBTITLE
Sodium Iodide Symporter Gene Transfer for Imaging and Ablation of Prostate Cancer

5. FUNDING NUMBERS
DAMD17-02-1-0119

6. AUTHOR(S) :
Sissy M. Jhiang, Ph.D.

7. PERFORMING ORGANIZATION NAME(S) AND ADDRESS(ES)
The Ohio State University Research Foundation
Columbus, Ohio 43210-1063

E-Mail: Jhiang.1@osu.edu

8. PERFORMING ORGANIZATION REPORT NUMBER

9. SPONSORING / MONITORING AGENCY NAME(S) AND ADDRESS(ES)
U.S. Army Medical Research and Materiel Command
Fort Detrick, Maryland 21702-5012

10. SPONSORING / MONITORING AGENCY REPORT NUMBER

11. SUPPLEMENTARY NOTES

12a. DISTRIBUTION / AVAILABILITY STATEMENT
Approved for Public Release; Distribution Unlimited

12b. DISTRIBUTION CODE

13. Abstract ***(Maximum 200 Words)*** *(abstract should contain no proprietary or confidential information)*

The sodium iodide symporter (NIS) mediates iodide uptake in thyroid follicular cells and provides a mechanism for effective radioiodide treatment of residual, recurrent, and metastatic thyroid cancers. The objective of the proposed research is to test the hypothesis that expression of exogenous hNIS in prostatic tissue will enable radioiodide to localize and ablate residual prostate cancer following prostatectomy, such that recurrence and metastasis of the disease can be prevented. The specific aims of this project are to: (1) confirm metastatic progression to distant lymph nodes and lungs following subcutaneous inoculation of rats with MATLyLu prostatic adenocarcinoma cells expressing hNIS; (2) investigate whether radioiodide therapy will prevent metastases and/or prolong survival in rats bearing subcutaneous MATLyLu tumors that express hNIS; (3) determine the expression level of hNIS required to elicit selective radioiodide-mediated killing of MATLyLu-hNIS prostatic adenocarcinoma cells *in vivo*; and, (4) restrict hNIS expression in prostatic tissue under transcriptional regulation of prostate-specific promoter.

14. SUBJECT TERMS:	15. NUMBER OF PAGES
prostate cancer, sodium iodide symporter, gene transfer, radioiodine	51
	16. PRICE CODE

17. SECURITY CLASSIFICATION OF REPORT	18. SECURITY CLASSIFICATION OF THIS PAGE	19. SECURITY CLASSIFICATION OF ABSTRACT	20. LIMITATION OF ABSTRACT
Unclassified	Unclassified	Unclassified	Unlimited

Table of Contents

INTRODUCTION

The sodium iodide symporter (NIS) mediates iodide uptake in thyroid follicular cells and provides a mechanism for effective radioiodide treatment of residual, recurrent, and metastatic thyroid cancers. The objective of the proposed research is to test the hypothesis that expression of exogenous hNIS in prostatic tissue will enable radioiodide to localize and ablate residual prostate cancer following prostatectomy, such that recurrence and metastasis of the disease can be prevented. The specific aims of this project are to: (1) confirm metastatic progression to distant lymph nodes and lungs following subcutaneous inoculation of rats with MATLyLu prostatic adenocarcinoma cells expressing hNIS; (2) investigate whether radioiodide therapy will prevent metastases and/or prolong survival in rats bearing subcutaneous MATLyLu tumors that express hNIS; (3) determine the expression level of hNIS required to elicit selective radioiodide-mediated killing of MATLyLu-hNIS prostatic adenocarcinoma cells *in vivo*; and, (4) restrict hNIS expression in prostatic tissue under transcriptional regulation of prostate-specific promoter.

BODY

Task 1. Confirm metastatic progression to distant lymph nodes and lungs following subcutaneous inoculation of rats with MATLyLu prostatic adenocarcinoma cells expressing hNIS

Appendix 1: KMD La Perle, D Shen, TLF Buckwalter, B Williams, A Haynam, G Hinkle, R Pozderac, CC Capen, and SM Jhiang (2002) "*In Vivo* Expression and Function of the Sodium Iodide Symporter Following Gene Transfer in the MATLyLu Rat Model of Metastatic Prostate Cancer", *The Prostate*, **50**: 170-178.

Appendix 2: KMD La Perle, EAG Blomme, CC Capen, and SM Jhiang (2003) "Effect of Exogenous Human Sodium/Iodide Symporter Expression on Growth of MatLyLu Cells", *Thyroid* in press

NIS gene transfer confers an increase of *In vitro* radioiodide-concentrating activity in a mixed population of MATLyLu-hNIS cells up to 72-fold. MATLyLu cells expressing NIS were injected subcutaneously in Copenhagen rats, which developed metastases in lymph nodes and lungs. NIS protein expression was confirmed in subcutaneous MATLyLu-hNIS tumors by immunohistochemistry and Western blot. Gamma counts of subcutaneous MATLyLu-hNIS tumors were 23-fold higher than parental MATLyLu tumors and radionuclide uptake in subcutaneous MATLyLu-hNIS tumors and lymph node metastases was visualized by whole-body image analysis.

We also showed that exogenous NIS expression decreased MATLyLu rat prostatic adenocarcinoma cell growth. Tumor growth and metastatic progression were significantly delayed in syngeneic rats injected with mixed or clonal populations of MATLyLu-NIS cells compared to rats bearing control tumors. MATLyLu-NIS tumors in

nude mice had a lower, albeit not statistically significant, growth rate than control tumors. The Ki-67 labeling index in NIS-positive areas was lower than in NIS-negative areas of rat tumors derived from a mixed population of MATLyLu-NIS cells. Growth of clonal populations of MATLyLu-NIS cells was delayed *in vitro*. These results demonstrate that NIS expression inhibits MATLyLu cell growth, thereby providing an additional potential benefit of NIS-mediated gene therapy for cancer.

Task 2. Investigate whether radioiodide therapy will prevent metastases and/or prolong survival in rats bearing subcutaneous MATLyLu tumors that express hNIS (Months 12-24, in progress)

Task 3. Determine the expression level of hNIS required to elicit selective radioiodide-mediated killing of MATLyLu-hNIS prostatic adenocarcinoma cells *in vivo* (Months 18-36, in progress)

Task 4. Restrict hNIS expression in prostatic tissue under transcriptional regulation of prostate-specific promoters (Months 1-36, in progress)

We are now in the process to construct recombinant adenovirus carrying PSA-hNIS. Once the recombinant adenovirus is available, we will perform radioiodide uptake assay and Western blot analysis of transduced LNCaP in the presence or absence of androgen stimulation. As negative controls, NIS expression will also be investigated in transduced PC-3 and NIH3T3 cells. Finally, whole body image analysis in athymic nude mice bearing LNCaP and PC-3 xenografts will be performed after intratumoral injection of recombinant adenovirus carrying PSA-hNIS.

KEY RESEARCH ACCOMPLISHMENTS

- Demonstrate *in vivo* expression and function of the sodium iodide symporter following *ex vivo* gene transfer in the MatLyLu rat model of metastatic prostate cancer.
- Discover expression of exogenous human sodium/iodide symporter inhibits growth of MatLyLu cells

REPORTABLE OUTCOMES

Manuscript 1: KMD La Perle, D Shen, TLF Buckwalter, B Williams, A Haynam, G Hinkle, R Pozderac, CC Capen, and SM Jhiang (2002) "*In Vivo* Expression and Function of the Sodium Iodide Symporter Following Gene Transfer in the MATLyLu Rat Model of Metastatic Prostate Cancer", *The Prostate*, **50**: 170-178.

Manuscript 2: KMD La Perle, EAG Blomme, CC Capen, and SM Jhiang (2003) "Effect of Exogenous Human Sodium/Iodide Symporter Expression on Growth of MatLyLu Cells", *Thyroid* in press

CONCLUSIONS

- NIS expression by a proportion of cells in a population was sufficient to confer radionuclide-concentrating function in subcutaneous and metastatic MATLyLu tumors. Ablation of residual normal and neoplastic prostate tissues by radioiodide after prostate-restricted NIS gene transfer might be a novel adjuvant therapy to prostatectomy for the treatment of advanced prostate cancer
- The finding that NIS expression inhibits MATLyLu cell growth, suggesting an additional potential benefit of NIS-mediated gene therapy for prostate cancer.

REFERENCES

See references listed in Appendix 1 and Appendix 2.

APPENDICES

Two manuscripts are appended.

The Prostate 50:170–178 (2002)
DOI 10.1002/pros.10046

In Vivo Expression and Function of the Sodium Iodide Symporter Following Gene Transfer in the MATLyLu Rat Model of Metastatic Prostate Cancer

Krista M.D. La Perle,[1] Daniel Shen,[2] Tara L.F. Buckwalter,[2] Bonnie Williams,[3] Aaron Haynam,[3] George Hinkle,[3] Rodney Pozderac,[3] Charles C. Capen,[1] and Sissy M. Jhiang[1,2]*

[1]Department of Veterinary Biosciences, The Ohio State University, Columbus, Ohio
[2]Departments of Physiology and Cell Biology, The Ohio State University, Columbus, Ohio
[3]Division of Nuclear Medicine, The Ohio State University, Columbus, Ohio

BACKGROUND. The sodium iodide symporter (NIS) mediates iodide uptake in thyroid follicular cells and provides a mechanism for effective radioiodide treatment of residual, recurrent, and metastatic thyroid cancers. This study investigated the clinical applications of NIS gene transfer for prostate cancer using the MATLyLu metastatic rat model.
METHODS. MATLyLu cells expressing NIS were injected subcutaneously in Copenhagen rats, which developed metastases in lymph nodes and lungs. NIS protein expression was evaluated by Western blot and immunohistochemistry, and function was measured by tissue gamma counts and whole-body imaging following radionuclide administration.
RESULTS. In vitro radioiodide-concentrating activity was increased up to 72-fold in a mixed population of MATLyLu-hNIS cells. NIS protein expression was confirmed in subcutaneous MATLyLu-hNIS tumors by immunohistochemistry and Western blot. Gamma counts of subcutaneous MATLyLu-hNIS tumors were 23-fold higher than parental MATLyLu tumors and radionuclide uptake in subcutaneous MATLyLu-hNIS tumors and lymph node metastases was visualized by whole-body image analysis.
CONCLUSIONS. NIS expression by a proportion of cells in a population was sufficient to confer radionuclide-concentrating function in subcutaneous and metastatic MATLyLu tumors. Ablation of residual normal and neoplastic prostate tissues by radioiodide after prostate-restricted NIS gene transfer might be a novel adjuvant therapy to prostatectomy for the treatment of advanced prostate cancer. *Prostate 50: 170–178, 2002.* © 2002 Wiley-Liss, Inc.

KEY WORDS: **NIS; MATLyLu; metastasis; prostate cancer; retrovirus; whole-body imaging**

INTRODUCTION

Prostate cancer is the leading cause of cancer and the second leading cause of cancer-related deaths annually in men in the United States and Europe [1]. The diagnosis can currently be made at an early stage because of prostate specific antigen (PSA) assays, which permit the detection of microscopic cancer during routine screening. However, localization and treatment of advanced invasive and metastatic prostate

Grant sponsor: Schering-Plough Research Institute; Grant sponsor: The Ohio State University (T32 Oncology Training Grant); Grant number: CA09228-23; Grant sponsor: American Cancer Society; Grant number: RPG-98-060-01-CCE.

*Correspondence to: Sissy M. Jhiang, Ph.D., The Ohio State University, 1645 Neil Avenue, 304 Hamilton Hall, Columbus, OH 43210. E-mail: Jhiang.1@osu.edu

Received 21 May 2001; Accepted 5 November 2001

cancer remains challenging [2]. Conventional treatment modalities for prostate cancer include radical prostatectomy, hormone deprivation therapy, and radiation therapy [3–5]. Although androgen deprivation is the only effective systemic therapy available for the treatment of locally advanced and metastatic prostate cancer [3], it eventually fails in most cases because of the progression of prostate cancer cells to androgen independence [6–8].

In contrast, residual, recurrent, and metastatic thyroid cancer has been effectively localized and ablated with radioiodide therapy following thyroidectomy [9]. Radioiodide therapy, which has been prescribed for virtually all thyroid cancer patients, has contributed to excellent 10-year survival rates, as well as low recurrence and mortality rates, with side-effects that are well tolerated [9]. Thyroid follicular epithelial cells have an inherent ability to concentrate iodide (I^-) in excess of 20–40-fold compared to the iodide concentration in plasma [10]. The sodium/iodide symporter (NIS), a 13 transmembrane glycoprotein localized on the basolateral membrane of thyroid follicular epithelial cells, mediates the active transport of one I^- ion and two sodium (Na^+) ions from the blood into follicular epithelial cells [10]. This translocation of I^- against its concentration gradient and Na^+ down its concentration gradient is driven by a Na^+/K^+ ATPase [10]. NIS function is hormonally regulated through thyrotropin (TSH) signaling [11], and specifically inhibited by perchlorate [10]. In addition to the thyroid gland, tissues such as salivary glands, gastric mucosa, and lactating mammary glands also have the capacity, albeit considerably lower than that of the thyroid gland, to accumulate iodide [10].

We have previously shown that active radioiodide uptake can be induced in non-thyroid cells in vitro by gene transfer of exogenous human NIS (hNIS) [12,13]. Subsequently, several studies have investigated the diagnostic and therapeutic applications of NIS gene transfer for various types of cancer in vivo primarily through the use of immunodeficient mice bearing subcutaneous cancer xenografts [13–18]. The aim of this study was to investigate the potential clinical applications of hNIS gene transfer for advanced prostate cancer using a biologically relevant model of metastatic prostate cancer. The Dunning (R-3327) rat model of prostate cancer was developed from a spontaneously occurring adenocarcinoma in a male Copenhagen rat [19]. Numerous cell lines that vary in their morphology, growth rate, hormone responsiveness, and metastatic potential were derived from this primary tumor [20]. The MATLyLu subline is a rapidly growing, androgen-independent, anaplastic cell line that is highly metastatic to lymph nodes and lungs following subcutaneous inoculation in syngeneic rats [21–23]. We have transduced MATLyLu cells with replication-defective retrovirus expressing hNIS to evaluate its impact on radioiodide-concentrating activity in vitro and in vivo.

MATERIALS AND METHODS

Generation of Recombinant hNIS Retrovirus

Recombinant retroviral DNA constructs containing either hNIS#9 cDNA or full-length hNIS (FLhNIS) cDNA were engineered using the retroviral vector LXSN (kindly provided by Dr. Kathleen Boris-Lawrie, The Ohio State University, Columbus, OH) to produce L-hNIS-SN. The protein encoded by hNIS#9 is truncated due to the absence of the last 31 amino acids at the C-terminus. Although this truncated protein is functional, available anti-hNIS antibodies recognize the C-terminus of the FLhNIS. L-hNIS-SN expresses hNIS cDNA under the control of the 5′ Moloney murine leukemia virus long terminal repeat promoter (L) and expresses a neomycin resistance gene (N) under the control of an internal Simian Virus 40 promoter (S) [24]. The retroviral packaging cell line, PA317 (American Type Culture Collection, ATCC, Manassas, VA) was maintained in Dulbecco's Modified Eagle Media with high glucose and L-glutamine, 10% fetal bovine serum, 100 U/ml penicillin G sodium and 100 μg/ml streptomycin sulfate. All cell culture media and reagents were purchased from Gibco-BRL Life Technologies, Inc., (Grand Island, NY) unless otherwise stated. Cells were transfected with 10 μg of either L-hNIS#9-SN, L-FLhNIS-SN or LXSN DNA using the calcium-phosphate precipitation method. Selection of transfectants was performed using 750 g/ml geneticin (G418) in the media for 5 days, followed by maintenance in media containing 350 g/ml G418. Starting 11 days post-transfection, individual drug-resistant PA317/L-hNIS#9-SN, PA317/L-FLhNIS-SN or PA317/LXSN clones were isolated. Individual clones, as well as mixed populations of transduced cells, were expanded and characterized by performing functional assays of iodide uptake. Viral supernatant was harvested every 12 hr until cells reached 80–100% confluency, centrifuged at 3,000*g* for 5 min at 4°C to remove cellular debris, and stored at −80°C. Virus harvested from PA317/hNIS cells that demonstrated the greatest radioiodide uptake activity in vitro was used to transduce MATLyLu cells.

Transduction of MATLyLu Cells

MATLyLu cells (generously provided by Dr. Albert A. Geldof from Academisch Ziekenhuis Vrije Universiteit, Amsterdam, The Netherlands) were main-

tained in RPMI-1640 supplemented with 10% fetal bovine serum, 100 U/ml penicillin G sodium, 100 μg/ml streptomycin sulfate, 2 mM L-glutamine, 1 mM sodium pyruvate, 10 mg/ml insulin, 5.5 mg/ml transferrin, and 6.7 μg/ml sodium selenite. Cells were transduced by incubation with 1 ml of filtered L-hNIS#9-SN, L-FLhNIS-SN or LXSN retrovirus in maintenance media for 24 hr. Selection of transduced MATLyLu cells was performed with 800 μg/ml G418 for 5 days followed by maintenance in 400 μg/ml G418. Individual clones, as well as mixed populations of transduced MATLyLu cells were expanded and characterized by performing functional assays of iodide uptake.

In Vitro Iodide Uptake Assays

NIS function for the various clones was evaluated by determining uptake of ^{125}I as previously described [12]. Briefly, 24-well plates were seeded with 5×10^4 to 5×10^5 parental, transfected, or transduced cells per well. Assays were performed in triplicate. Twenty-four hours later, cells were incubated with 2 μCi of ^{125}I (Amersham Pharmacia Biotech, Piscataway, NJ) in cold NaI for 30 min at 37°C. Cells were then rapidly washed twice with 1 ml of Hanks Balanced Salt Solution (HBSS), and incubated in 1 ml of 95% ethanol at room temperature for 20 min. The supernatant was counted in a Cobra auto-γ-radiation counter (Packard Instrument Co., Meriden, CT). To demonstrate perchlorate inhibition, 10 μl of 3 mM $NaClO_4$ was added immediately following addition of ^{125}I.

MATLyLu Animal Model of Metastasis

Two to three-month old male Copenhagen rats were obtained from Harlan-Sprague Dawley (Indianapolis, IN). Rats were allowed ad libitum access to water and standard rodent chow, and were monitored daily. All experimental procedures received approval from the Institutional Laboratory Animal Care and Use Committee of The Ohio State University. Rats were injected subcutaneously in the right flank with 1×10^6 parental or transduced MATLyLu cells suspended in 0.5 ml of HBSS. Tumor progression was monitored daily by palpation and assessment of respiratory rate. Tumor size at the site of injection was measured with microcalipers weekly and at necropsy, and tumor volumes were calculated in cubic centimeters using the equation: volume = length × width × height × 0.5236 [25].

Ex Vivo Tissue Gamma Counts

Eleven days following inoculation with parental MATLyLu or transduced MATLyLu-FLhNIS cells, rats were injected in the lateral tail vein with 10 μCi ^{123}I in phosphate buffered saline, and killed 8 hr later. Normal tissues (thyroid gland, stomach, salivary gland, lung, liver, and spleen) and subcutaneous tumors were collected to measure radioactivity in a γ-counter. The data were presented as a fold increase in radioactivity of respective tissues, compared with spleen according to the following formula: (counts of tissue of interest/gm of tissue of interest)/(counts of spleen/gm of spleen).

Immunohistochemical Staining and Western Blot Analysis

Complete necropsies and histopathological evaluations were performed on all animals. Portions of parental and transduced MATLyLu tumors were fixed in 10% neutral-buffered formalin, routinely processed, and embedded in paraffin. Immunohistochemical staining was performed as reported previously with several modifications [26]. Tissue sections (5 μm) were incubated with an anti-hNIS proprietary polyclonal rabbit antibody (#331, 1:500 dilution) at room temperature for 1 hr, and then incubated with biotinylated goat anti-rabbit IgG (1:200 dilution, Santa Cruz Biotechnology, Santa Cruz, CA) for 20 min. Western blot analysis of membrane proteins prepared from tumor pieces frozen in liquid nitrogen was also performed as previously described [27]. Briefly, the transferred filters were incubated with the proprietary anti-hNIS antibody (#331, 1:1,500 dilution) for 1 hr at room temperature, followed by incubation with horseradish peroxidase-conjugated donkey anti-rabbit IgG (1:5,000 dilution, Amersham Pharmacia Biotech) for 1 hr at room temperature.

Whole-Body Image Analysis

Between 10 and 33 days following subcutaneous inoculation of parental or transduced MATLyLu cells, rats were anesthetized with Ketamine HCl (Fort Dodge, Fort Dodge, IA) and Xylazine (Fort Dodge), and then placed in a prone position on a gamma camera (Picker Prism 2000XP Baseline V8.5A, dual-head, gantry-fixed, PCD- and SPECT-capable, Marconi Medical Systems, Cleveland, OH) fitted with a low energy, ultra high resolution, planar collimator (ventral-dorsal view) and a pinhole collimator (dorsal-ventral view) interfaced to a computer-based nuclear medicine imaging system (Odyssey VP, Marconi Medical Systems). Rats were injected in the lateral tail vein with 0.2 ml of a saline solution containing 3 mCi of $^{99m}TcO_4$ (also a substrate for NIS) or 300 μCi ^{123}I (Amersham Pharmacia Biotech). Serial static images were obtained 5, 20, and 60 min post-injection of the radionuclide with an acquisition time appropriate for

500–1000K pre-set total counts but less than 5 min to reduce motion artifact.

Statistical Analysis

Numerical data were expressed as means ± the standard error of the mean (SEM). Statistical differences between means for different data sets were evaluated with GraphPad Instat version 3.0 (GraphPad software, San Diego, CA) using one-way analysis of variance (ANOVA) and Tukey-Kramer multiple comparisons test. Statistical significance was indicated by $P < 0.001$.

RESULTS

In Vitro Radioiodide-Concentrating Activity

MATLyLu-hNIS#9 cells demonstrated radioiodide uptake activities (RAIU) that were 30–40-fold higher than those of non-transduced parental cells (Fig. 1A). In addition, the RAIU for a mixed population of MATLyLu-hNIS#9 cells was comparable to four different clonal MATLyLu-hNIS#9 populations. Transduction of MATLyLu cells with retrovirus expressing FLhNIS also resulted in a marked increase (up to 72-fold, data not shown) in RAIU compared to non-transduced parental MATLyLu cells or MATLyLu cells transduced with vector only (LXSN) retrovirus (Fig. 1B). The induced RAIU in MATLyLu cells expressing FLhNIS was also specifically inhibited by perchlorate (Fig. 1B). Given the fact that exogenous genes may not be delivered to every cell in a target population in human gene therapy clinical trials, mixed populations of MATLyLu-FLhNIS cells were used for the in vivo studies below.

In Vivo Tumor Formation

Following subcutaneous inoculation in the right flank with parental MATLyLu or transduced MATLyLu-FLhNIS cells, Copenhagen rats consistently developed metastases in distant lymph nodes and lungs (Fig. 2). Subcutaneous tumors and ipsilateral axillary lymph node metastases were palpable by 7 and 25 days post-injection (d.p.i.), respectively. Widespread 2–3 mm lung metastases were present by 30 d.p.i. at which time rats became dyspneic and were euthanized.

Ex Vivo hNIS Function and Protein Expression

To assess the functional activity of NIS, rats were injected intravenously with 10 μCi ^{123}I 11 days following inoculation with parental MATLyLu or transduced MATLyLu-FLhNIS cells. Radioiodide uptake activity was measured in normal tissues and subcutaneous tumors with a γ-counter. Ex vivo γ-counts for subcutaneous MATLyLu-FLhNIS tumors were 23-fold higher than those of the spleen, while γ-counts for parental MATLyLu tumors were comparable to those of the spleen (Fig. 3). Although MATLyLu-FLhNIS tumor γ-counts were considerably less than those of the thyroid gland, they were higher than those of the stomach and salivary gland, which are tissues with high levels of endogenous NIS expression. NIS protein expression was also confirmed in MATLyLu-FLhNIS tumors by Western blot and immunohistochemistry. NIS protein, indicated by a 90 kDa glycopeptide and a 60 kDa partially glycosylated peptide, was present in membrane fractions from MATLyLu-FLhNIS tumors (Fig. 4). By immunohistochemistry, large numbers of cells with intensely positive membrane staining were interspersed with unstained cells in MATLyLu-FLhNIS tumors (Fig. 5). This staining pattern is consistent for tumors derived from a mixed population of transduced MATLyLu-FLhNIS cells.

In Vivo Radionuclide Uptake

To determine whether NIS function was sufficient for the in vivo detection of radionuclide by transduced tumor cells, whole-body images were non-invasively obtained. Primary subcutaneous MATLyLu-FLhNIS tumors and ipsilateral axillary lymph node metastases, but not MATLyLu-LXSN tumors were visualized by whole-body imaging following administration of radionuclide (Fig. 6). All subcutaneous MATLyLu-FLhNIS tumors that were imaged with $^{99m}TcO_4$ or ^{123}I were detected as early as 10 d.p.i. Twelve rats with MATLyLu-FLhNIS tumors had axillary lymph node metastases but only three of these were detectable as early as 25 d.p.i. by whole-body imaging. Ten of these rats had lung metastases, which were macroscopically visible in three rats but only microscopically apparent in seven rats; none of the lung metastases was detected by whole-body imaging.

DISCUSSION

The results of this study demonstrate that retroviral-mediated expression of FLhNIS conferred radionuclide-concentrating activity in the MATLyLu model of metastatic prostate cancer. Subcutaneous inoculation of a mixed population of MATLyLu-FLhNIS cells resulted in the formation of tumors with functional NIS expression. Distant metastases to ipsilateral axillary lymph nodes and lungs also developed; however, only lymph node metastases could be visualized by whole-body imaging.

Previous studies have investigated the utility of NIS gene transfer to facilitate radioiodide therapy of thyroid cancers that have lost the ability to concentrate radioiodide [28], or non-thyroidal cancers that lack

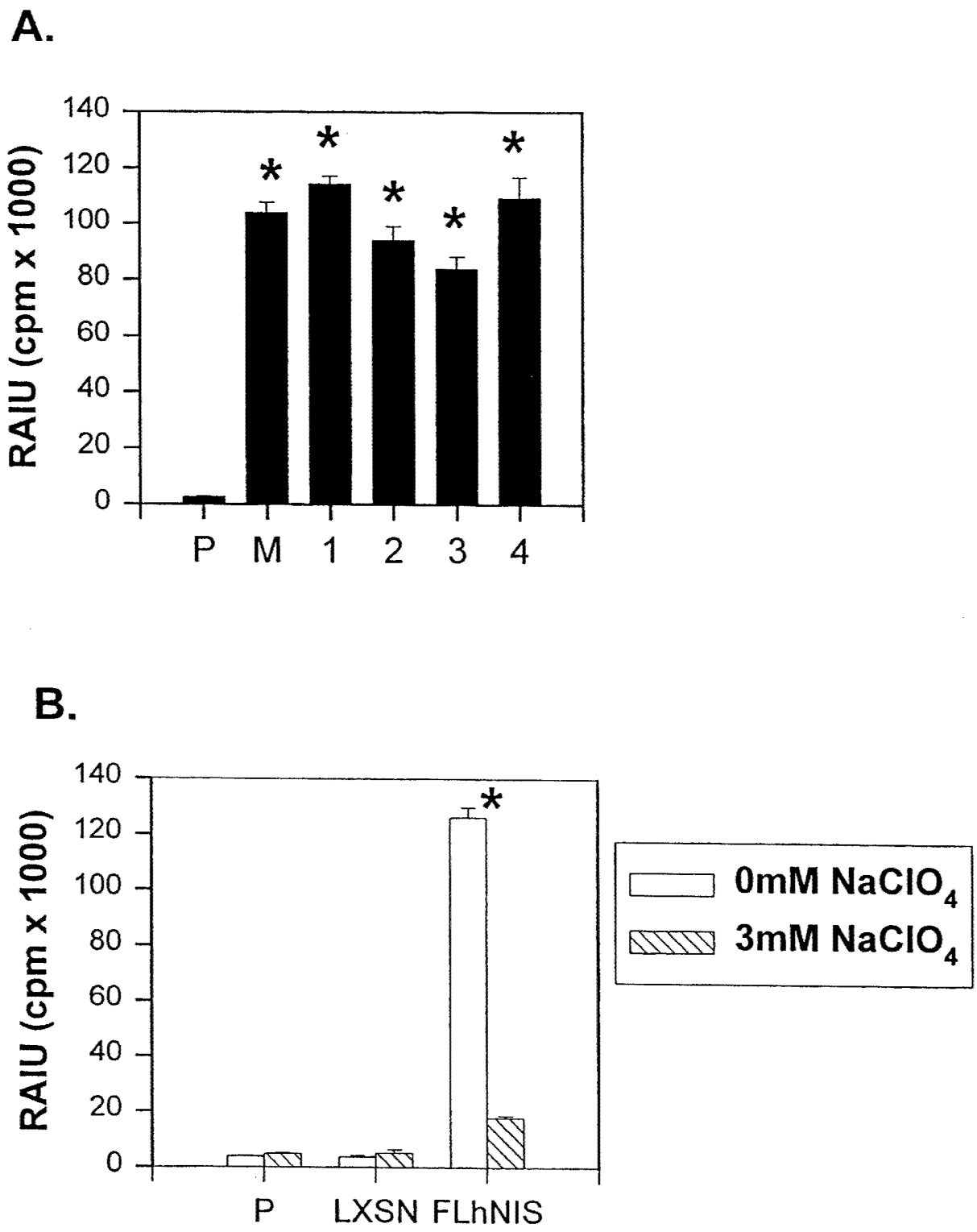

Fig. 1. Radioiodide uptake activities (RAIU) of MATLyLu cells transduced with retrovirus expressing hNIS. **A**: Four individual clones and a mixed population (M) of MATLyLu-hNIS#9 cells demonstrated 30 – 40-fold higher RAIU than non-transduced parental cells (P). N = 3. *Significantly different ($P < 0.001$). **B**: RAIU for a mixed population of MATLyLu-FLhNIS cells was 32-fold higher than non-transduced parental cells (P) or cells transduced with empty vector retrovirus (LXSN). RAIU was inhibited 7-fold by the addition of sodium perchlorate ($NaClO_4$). N = 3. $P < 0.001$.

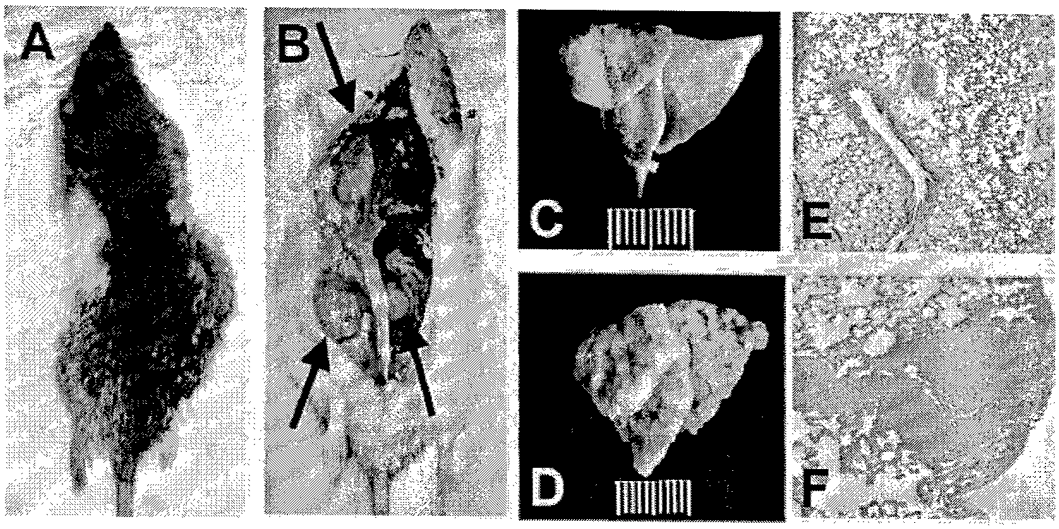

Fig. 2. Regional and distant metastases in Copenhagen rats injected with MATLyLu-FLhNIS cells. **A**: Large subcutaneous tumor in the right flank 33 days after subcutaneous injection of 1×10^6 MATLyLu-FLhNIS cells. **B**: Multiple lymph nodes with metastases (arrows) 33 days post-injection. **C** and **D**: Left lung lobes from a rat with no macroscopically visible lung metastases (C) and from a rat with numerous 2–3 mm metastases 33 days post-injection (D). **E** and **F**: Histologic appearance of the lungs pictured in C (E) and D (F) (hematoxylin and eosin, × 200).

endogenous radioiodide-concentrating ability [13–18]. Most of the in vivo models used in these studies have been athymic nude mice bearing subcutaneous human and animal cancer xenografts. For some types of human cancers, these models are often the only animal models available for investigating tumorigenesis and therapeutic approaches. However, these models are artificial in that the biological processes involved in tumor formation and the host cellular responses to the xenografts do not recapitulate those of spontaneous tumors arising in immune competent hosts [29–31]. Furthermore, most xenograft models do not naturally develop metastases unless cancer

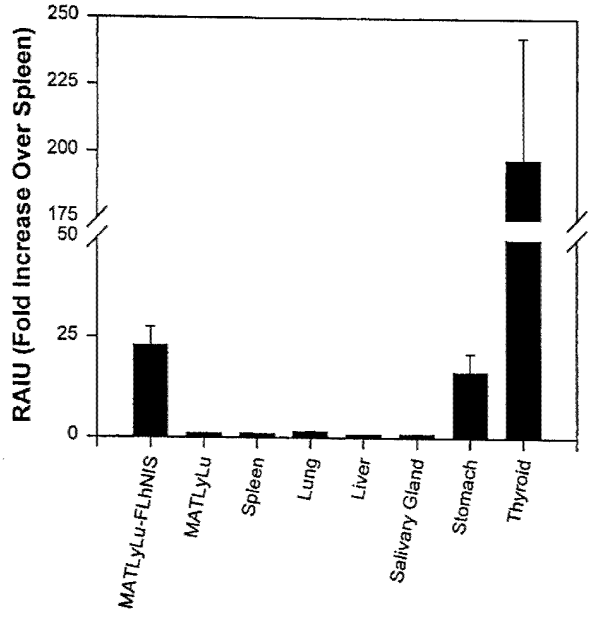

Fig. 3. Ex vivo tissue γ-counts for rats with subcutaneous parental MATLyLu-FLhNIS or MATLyLu tumors (Day 11) 8 hr following injection with 10 μCi ^{123}I. Radioiodide uptake activities (RAIU) of MATLyLu-FLhNIS tumor pieces were 23-fold higher than those of the spleen. Values for the thyroid gland, stomach, and salivary gland which have high endogenous NIS expression are included as positive controls while values for the lung and liver are included as negative controls. N = 4.

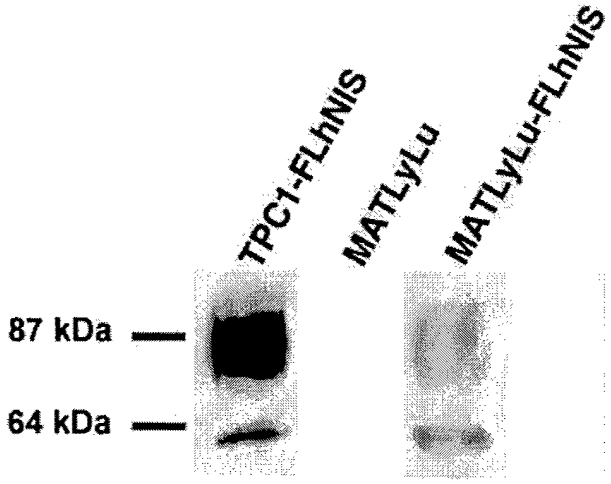

Fig. 4. Western blot analysis of membrane fraction protein isolated from parental MATLyLu or transduced MATLyLu-FLhNIS tumor pieces. Note the mature glycopeptide (90 kDa) and the partially glycosylated peptide (60 kDa). TPCI-FLhNIS, consisting of membrane fraction protein harvested from TPC-1 papillary thyroid carcinoma cells transduced with L-FLhNIS-SN retrovirus, is included as a positive control.

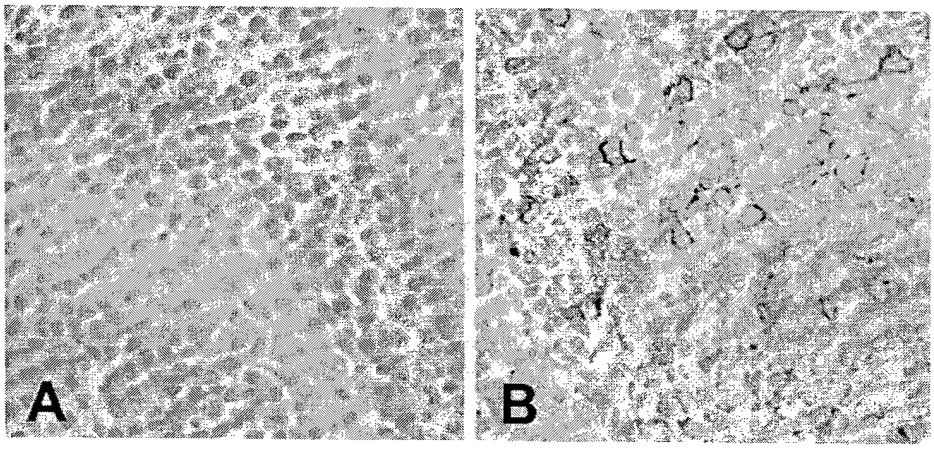

Fig. 5. Immunohistochemical stain for hNIS in parental MATLyLu (**A**) and transduced MATLyLu-FLhNIS (**B**) tumor pieces. Positive membrane staining is apparent in large numbers of MATLyLu-FLhNIS cells interspersed with unstained cells; this staining pattern is consistent for tumors that are derived from a mixed population of retrovirally-transduced cells (avidin-biotin complex immunoperoxidase method, hematoxylin counterstain, × 200).

cells are injected orthotopically [29,30,32]. Rodents that develop tumors in the lung following tail vein injection with cancer cells are often labeled as metastatic models, although tumor formation at this site is merely due to passage through this first vascular bed encountered after the tail vein and does not recapitulate the entire metastatic cascade [30,31]. Although tumors are highly aggressive and do not metastasize to bone in the subcutaneous MATLyLu model, this model is unique in that metastases consistently develop in distant sites from a subcutaneous xenograft by natural lymphatic invasion [21–23].

Use of a mixed population of MATLyLu-FLhNIS cells for these in vivo studies biologically mimics the scenario in human gene therapy trials in which clinicians are limited in their ability to transfer exogenous genes to every cell in a target population. We were able to demonstrate radioiodide-concentrating activity in a

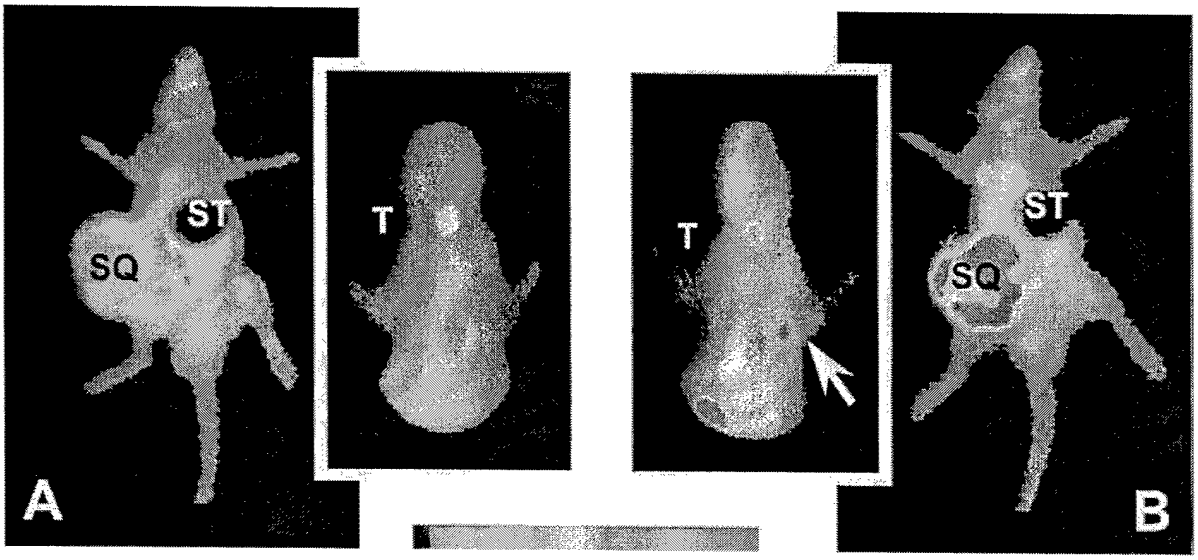

Fig. 6. Whole-body images of rats with MATLyLu-LXSN (**A**) or MATLyLu-FLhNIS (**B**) tumors (Day 25). Images were obtained 1 hr following administration of 3 mCi of $^{99m}TcO_4$ in the tail vein. A lead disk was placed over the region of the stomach (ST). Radionuclide uptake by the thyroid (T) is evident in both rats. There is central necrosis of the subcutaneous tumors (SQ), which is surrounded by a peripheral rim of viable tissue. Intense uptake of $^{99m}TcO_4$ by the subcutaneous tumor and the ipsilateral axillary lymph node metastasis (arrow) is only visible in the rat injected with MATLyLu-FLhNIS cells. Color bar indicates radionuclide uptake that increases in intensity from black to red.

mixed population of retrovirally-transduced cancer cells. Furthermore, successful imaging of distant MATLyLu-FLhNIS lymph node metastases derived from a mixed population of transduced cells indicated that hNIS expression by only a proportion of cells in a tumor is sufficient to confer radionuclide-concentrating function. Taken together, these results demonstrate the potential of gene therapy in spite of suboptimal transfer efficiency.

The detection by whole-body imaging of MATLyLu-FLhNIS lymph node metastases in only 3/12 rats following radionuclide administration suggests that a certain level of NIS expression is necessary to confer radionuclide-concentrating function. When considering tumors derived from a mixed population of transduced MATLyLu-FLhNIS cells, the in vitro radioiodide-concentrating activity represents an average for cells expressing different levels of NIS. Consequently, inherent tumor heterogeneity [30,33] was exaggerated by the fact that heterogeneous cells were used for animal injections. It is also possible that tumor cells expressing lower levels of hNIS have a growth advantage and/or metastasize more readily. Factors such as tumor size, necrosis, blood flow, and pressure might be responsible for the lack of radionuclide uptake in 9/12 MATLyLu-FLhNIS lymph node metastases [33]. However, some metastases not visible by whole-body imaging were similar in size to metastases that were visible. In addition, extensive necrosis generally was not detected in lymph node metastases by histopathological evaluation. Lack of uptake by lymph node metastases could also be due to rapid efflux of the radionuclide before the acquisition of images between 5 and 60 min following administration. But, images were acquired every 20–60 sec for 5 min immediately upon intravenous injection of the radionuclide in some animals, and uptake was still not evident in lymph node metastases.

The results of this study illustrate the potential clinical applications of hNIS gene therapy for prostate cancer. The best therapeutic strategy for patients with cancer is to maximize the efficacy of the initial treatment when the disease is still confined to the prostate gland [8,34]. Given the current state of gene delivery strategies, hNIS-based radioiodide therapy for prostate cancer will be most effective for the treatment of locally invasive cancer in which the lesion is often difficult to be excised completely with surgery. Similar to the clinical approach for patients with thyroid cancer, the dispensability of the prostate gland allows aggressive initial treatment of the cancer with total prostatectomy followed potentially by ablation of residual normal and neoplastic prostate tissues by radioiodide after prostate-restricted hNIS gene transfer [17,35–37]. Complete ablation of prostate tissue would increase the sensitivity of using serum PSA levels to monitor for recurrence and metastasis [34]. Sodium/iodide symporter-based radioiodide therapy could also be used to monitor for local recurrence, as well as detect and treat metastatic cancer. However, these latter applications are dependent on future advances in systemic gene delivery. Current studies are investigating the effect of ^{131}I on interrupting tumor progression and preventing the development of metastases in the MATLyLu model.

ACKNOWLEDGMENTS

We thank Dr. Albert A. Geldof from Academisch Ziekenhuis Vrije Universiteit, Amsterdam, The Netherlands for providing the MATLyLu cells, Dr. Kathleen Boris-Lawrie for providing the LXSN retroviral vector, Dr. Richard Kloos for scientific discussion, Ms. Kathy Hopwood for superior animal husbandry, Ms. Heather Caprette and Mr. Marc Hardman for assistance with photography and figure illustrations, and Ms. Anjli Venkateswaran, Ms. Danielle Westfall, and Mr. Marc Lavender for assistance with animal injections and postmortem evaluations. This project was supported in part by a fellowship from the Schering-Plough Research Institute (KMDL, CCC), T32 Oncology Training Grant CA09228-23 from The Ohio State University, Comprehensive Cancer Center, Department of Internal Medicine, Division of Hematology and Oncology (KMDL), and by American Cancer Society grant RPG-98-060-01-CCE (SMJ).

REFERENCES

1. Greenlee RT, Hill-Harmon MB, Murray T, Thun M. Cancer statistics, 2001. CA Cancer J Clin 2001;51:15–36.
2. Zippe CD, Kedia AW. Locally invasive prostate cancer: An evolving concept of advanced disease. In: Klein EA, editor. Management of prostate cancer. Totawa: Humana Press; 2000. p 223–243.
3. Hahnfeld LE, Moon TD. Prostate cancer. Med Clin North Am 1999;83:1231–1245.
4. Freid RM, Davis NS, Weiss GH. Prostate cancer screening and management. Med Clin North Am 1997;81:801–822.
5. Small EJ. Prostate cancer: Incidence, management and outcomes. Drugs Aging 1998;13:71–81.
6. Koivisto P, Kolmer M, Visakorpi T, Kallioniemi OP. Androgen receptor gene and hormonal therapy failure of prostate cancer. Am J Pathol 1998;152:1–9.
7. Sadar MD, Hussain M, Bruchovsky N. Prostate cancer: Molecular biology of early progression to androgen independence. Endoct Relat Cancer 1999;6:487–502.
8. Mason MD. Prostate Cancer. In: Jiang WG, Mansel RE, editors. Cancer metastasis, molecular and cellular mechanisms and clinical intervention. Dordrecht: Kluwer Academic Publishers; 2000. p 279–296.
9. Mazzaferri EL. Radioiodine and other treatments and outcomes. In: Braverman LE, Utiger RD, editors. Werner and ingbar's The Thyroid: A fundamental and clinical text. Eighth

edition. Philadelphia: Lippincott Williams and Wilkins; 2000. p 904–929.

10. Carrasco N. Iodide transport in the thyroid gland. Biochim Biophys Acta 1993;1154:65–82.
11. Kaminsky SM, Levy O, Salvador C, Dai G, Carrasco N. Na^+-I^- symport activity is present in membrane vesicles from thyrotropin-deprived non-I^--transporting cultured thyroid cells. Proc Natl Acad Sci U S A 1994;91:3789–3793.
12. Smanik PA, Liu Q, Furminger TL, Ryu K, Xing S, Mazzaferri EL, Jhiang SM. Cloning of the human sodium iodide symporter. Biochem Biophys Res Commun 1996;226:339–345.
13. Cho JY, Xing S, Liu X, Buckwalter TL, Hwa L, Sferra TJ, Chiu IM, Jhiang SM. Expression and activity of human Na^+/I^- symporter in human glioma cells by adenovirus-mediated gene delivery. Gene Ther 2000;7:740–749.
14. Mandell RB, Mandell LZ, Link CJ, Jr. Radioisotope concentrator gene therapy using the sodium/iodide symporter gene. Cancer Res 1999;59:661–668.
15. Nakamoto Y, Saga T, Misaki T, Kobayashi H, Sato N, Ishimori T, Kosugi S, Sakahara H, Konishi J. Establishment and characterization of a breast cancer cell line expressing Na^+/I^- symporters for radioiodide concentrator gene therapy. J Nucl Med 2000;41:1898–1904.
16. Boland A, Ricard M, Opolon P, Bidart JM, Yeh P, Filetti S, Schlumberger M, Perricaudet M. Adenovirus-mediated transfer of the thyroid sodium/iodide symporter gene into tumors for a targeted radiotherapy. Cancer Res 2000;60:3484–3492.
17. Spitzweg C, O'Connor MK, Bergert ER, Tindall DJ, Young CY, Morris JC. Treatment of prostate cancer by radioidine therapy after tissue-specific expression of the sodium iodide symporter. Cancer Res 2000;60:6526–6530.
18. Haberkorn U, Henze M, Altmann A, Jiang S, Morr I, Mahmut M, Peschke P, Kubler W, Debus J, Eisenhut M. Transfer of the human Nal symporter gene enhances iodide uptake in hepatoma cells. J Nucl Med 2001;42:317–325.
19. Dunning WF. Prostate cancer in the rat. Monogr Natl Cancer Inst 1963;12:351–369.
20. Isaacs JT, Isaacs WB, Feitz WF, Scheres J. Establishment and characterization of seven Dunning rat prostatic cancer cell lines and their use in developing methods for predicting metastatic abilities of prostatic cancers. Prostate 1986;9:261–281.
21. Isaacs JT, Yu GW, Coffey DS. The characterization of a newly identified, highly metastatic variety of Dunning R 3327 rat prostatic adenocarcinoma system: The MAT LyLu tumor. Invest Urol 1981;19:20–23.
22. Geldof AA, Rao BR. Factors in prostate cancer metastasis. Anticancer Res 1990;10:1303–1306.
23. Vieweg J, Heston WD, Gilboa E, Fair WR. An experimental model simulating local recurrence and pelvic lymph node metastasis following orthotopic induction of prostate cancer. Prostate 1994;24:291–298.
24. Miller AD, Rosman GJ. Improved retroviral vectors for gene transfer and expression. Biotechniques 1989;7:980–990.
25. Janik P, Briand P, Hartmann NR. The effect of estrone-progesterone treatment on cell proliferation kinetics of hormone-dependent GR mouse mammary tumors. Cancer Res 1975;35: 3698–3704.
26. Jhiang SM, Cho JY, Ryu KY, DeYoung BR, Smanik PA, McGaughy VR, Fischer AH, Mazzaferri EL. An immunohistochemical study of Na^+/I^- symporter in human thyroid tissues and salivary gland tissues. Endocrinology 1998;139:4416–4419.
27. Cho JY, Leveille R, Kao R, Rousset B, Parlow AF, Burak WE, Jr., Mazzaferri EL, Jhiang SM. Hormonal regulation of radioiodide uptake activity and Na^+/I^- symporter expression in mammary glands. J Clin Endocrinol Metab 2000;85:2936–2943.
28. Smit JW, Shroder-van der Elst JP, Karperien M, Que I, van der Pluijm G, Goslings B, Romijn JA, van der Heide E. Reestablishment of in vitro and in vivo iodide uptake by transfection of the human sodium iodide symporter (hNIS) in a hNIS defective human thyroid carcinoma cell line. Thyroid 2000;10:939–943.
29. Mitchell BS, Schumacher U. Use of immunodeficient mice in metastasis research. Br J Biomed Sci 1997;54:278–286.
30. Welch DR. Technical considerations for studying cancer metastasis in vivo. Clin Exp Metastasis 1997;15:272–306.
31. McClatchey AE. Modeling metastasis in the mouse. Oncogene 1999;18:5334–5339.
32. Reiter RE, Sawyers CL. Xenograft models and the molecular biology of human prostate cancer. In: Chung LWK, Isaacs WB, Simons JW, editors. Prostate cancer: Biology, genetics, and the new therapeutics. Totowa: Humana Press; 2001. p 163–174.
33. Dvorak HF, Nagy JA, Feng D, Dvorak AM. Tumor architecture and targeted delivery. In: Abrams PG, Fritzberg AR, editors. Radioimmunotherapy of cancer. Seattle: NeoRx; 2000. p 107–135.
34. Tefilli MV, Gheiler EL, Pontes JE. Management of recurrent diseases after definitive therapy. In: Klein EA, editor. Management of prostate cancer. Totowa: Humana Press; 2000. p 245–263.
35. Pang S, Taneja S, Dardashti K, Cohan P, Kaboo R, Sokoloff M, Tso C-L, deKernion JB, Belldegrun AR. Prostate tissue specificity of the prostate-specific antigen promoter isolated from a patient with prostate cancer. Hum Gene Ther 1995;6:1417–1426.
36. Pang S, Sannull J, Kaboo R, Xie Y, Tso C-L, Michel K, deKernion JB, Belldegrun AR. Identification of a positive regulatory element responsible for tissue-specific expression of prostate-specific antigen. Cancer Res 1997;57:495–499.
37. Spitzweg C, Zhang S, Bergert ER, Castro MR, Mclver B, Heufelder AE, Tindall DJ, Young CY, Morris JC. Prostate-specific antigen (PSA) promoter-driven androgen-inducible expression of sodium iodium iodide symporter in prostate cancer cell lines. Cancer Res 1999;59:2136–2141.

EFFECT OF EXOGENOUS HUMAN SODIUM/IODIDE SYMPORTER EXPRESSION ON GROWTH OF MATLyLu CELLS

Krista M. D. La Perle[1], Eric A. G. Blomme[2], Charles C. Capen[1], and Sissy M. Jhiang[1,3]

[1]Departments of Veterinary Biosciences and [3]Physiology and Cell Biology, The Ohio State University, Columbus, OH, USA and [2]Pharmacia, Skokie, IL, USA

This project was supported in part by a fellowship from the Schering-Plough-Research Institute (K. M. D. L., C. C. C.), Institutional National Research Service Award T32 CA09228-23 from The Ohio State University, Comprehensive Cancer Center, Department of Internal Medicine, Division of Hematology and Oncology (K. M. D. L.), and U.S. Army Medical Research and Material Command Department of Defense 2001 Prostate Cancer Research Program PC010162 (S. M. J.).

Running Title: hNIS Expression Decreases MATLyLu Growth

Key Words: Gene therapy, Growth, Metastasis, Na^+/I^- Symporter, Retrovirus

Corresponding Author: Sissy M. Jhiang, Ph.D., The Ohio State University, Department of Physiology and Cell Biology, 304 Hamilton Hall, 1645 Neil Avenue, Columbus, OH 43210, Phone: 614-292-4312, Fax: 614-292-4888, Email: Jhiang.1@osu.edu.

ABSTRACT

The sodium/iodide symporter (NIS) mediates iodide uptake in thyroid cells and enables the effective radioiodide treatment of thyroid cancers. There is much interest to facilitate radioiodide therapy in other cancers by NIS gene transfer. This study showed that exogenous NIS expression decreased MATLyLu rat prostatic adenocarcinoma cell growth. Tumor growth and metastatic progression were significantly delayed in syngeneic rats injected with mixed or clonal populations of MATLyLu-NIS cells compared to rats bearing control tumors. MATLyLu-NIS tumors in nude mice had a lower, albeit not statistically significant, growth rate than control tumors. The Ki-67 labeling index in NIS-positive areas was lower than in NIS-negative areas of rat tumors derived from a mixed population of MATLyLu-NIS cells. Growth of clonal populations of MATLyLu-NIS cells was delayed *in vitro*. These results demonstrate that NIS expression inhibits MATLyLu cell growth, thereby providing an additional potential benefit of NIS-mediated gene therapy for cancer.

INTRODUCTION

The inherent ability of the thyroid gland to transport iodide is mediated by the sodium (Na^+)/iodide (I^-) symporter (NIS) (1). This 13 transmembrane glycoprotein present on the basolateral membrane of thyroid follicular epithelial cells couples the inward movement of two Na^+ ions with one I^- ion in an active process driven by a Na^+/K^+ ATPase (1). Consequently, the thyroidal intracellular concentration of I^- is 20-40-fold higher than that in the plasma (1). This uptake of I^- is a crucial step in the production of the thyroid hormones, tri-iodothyronine (T_3) and tetra-iodothyronine or thyroxine (T_4). In addition, this aspect of normal thyroid physiology has been successfully exploited for the localization and ablation of residual, recurrent and metastatic thyroid cancer subsequent to radionuclide administration. The standard therapeutic regimen for thyroid cancer, which combines thyroidectomy followed by radioiodide therapy, has contributed to excellent 10-year survival rates and low recurrence and mortality rates with minimal side effects (2).

As a result of this success in treating thyroid cancer, gene therapy strategies employing NIS have become attractive for the treatment of various types of cancer. In recent years, several studies have investigated the clinical applications of either rat (rNIS) or human (hNIS) NIS gene transfer by non-viral and viral methods for *in vitro* cell killing, *in vivo* imaging, and/or radioiodide therapy of cervical, breast, hepatic, thyroid, and prostate cancer, and melanoma xenografts in rodents (3-11). The majority of these studies have utilized

immunodeficient mice bearing subcutaneous human cancer xenografts (3,4,6,8,10,11), with fewer studies using syngeneic rat models (5,7,9). We recently reported the detection of subcutaneous tumors and metastases in lymph nodes by nuclear scintigraphy following *ex vivo* retroviral gene transfer of hNIS in the MATLyLu syngeneic rat model of metastatic prostate cancer (9). During the course of this study, we observed that NIS-transduced tumors were smaller and progressed at a slower rate *in vivo* than parental or vector-transduced tumors. The aim of the current study was to explore this further and determine the effect of hNIS expression on the growth of MATLyLu rat prostatic adenocarcinoma cells *in vitro* and *in vivo* in the absence of radioiodide therapy.

MATERIALS and METHODS

Recombinant hNIS Retrovirus

Recombinant retroviral DNA constructs containing either hNIS#9 cDNA or FLhNIS cDNA were engineered using the retroviral vector LXSN (kindly provided by Dr. Kathleen Boris-Lawrie, The Ohio State University, Columbus, OH) to produce L-hNIS-SN. The protein encoded by hNIS#9 is truncated due to the absence of the last 31 amino acids at the C-terminus. This truncated protein is functional; however, available anti-hNIS antibodies recognize the C-terminus of the FLhNIS. L-hNIS-SN expresses hNIS cDNA under the control of the 5' Moloney murine leukemia virus long terminal repeat promoter (L) and expresses

a neomycin resistance gene (N) under the control of an internal Simian Virus 40 promoter (S) (12). Retrovirus was generated as previously described (9).

MATLyLu Cells and Syngeneic Copenhagen Rat Animal Model

The MATLyLu cell line is one of several sublines developed from a spontaneous prostatic adenocarcinoma in a Copenhagen rat (13). The MATLyLu subline is a rapidly growing, androgen-independent, anaplastic cell line that is highly metastatic to ipsilateral lymph nodes and lungs following subcutaneous injection in syngeneic Copenhagen rats (14-16). MATLyLu cells were obtained from Dr. Laurie K. McCauley (Department of Periodontics/Prevention/Geriatrics, University of Michigan, Ann Arbor, MI), the European Collection of Cell Cultures (ECACC, #94101454, Salisbury, Wiltshire, United Kingdom), and Dr. Albert A. Geldof (Academisch Ziekenhuis Vrije Universiteit, Amsterdam, The Netherlands), and were maintained in RPMI-1640 supplemented with 10% fetal bovine serum, 100 U/ml penicillin G sodium, 100 μg/ml streptomycin sulfate, 2 mM L-glutamine, 1 mM sodium pyruvate, 10 mg/ml insulin, 5.5 mg/ml transferrin, and 6.7 μg/ml sodium selenite. All cell culture media and reagents were purchased from Gibco-BRL Life Technologies, Inc. (Grand Island, NY) unless otherwise stated. Cells were transduced by incubation with 1 ml of filtered L-hNIS#9-SN, L-FLhNIS-SN, or LXSN retrovirus in maintenance media for 24 hr. Selection of transduced MATLyLu cells was performed with 800 μg/ml Geneticin (G418) for 5 days followed by maintenance in 400 μg/ml G418. Individual clones, as well as mixed populations of transduced MATLyLu cells were expanded and used for *in vitro*

and *in vivo* studies. NIS expression in transduced cells was confirmed *in vitro* by iodide uptake assays as previously reported (9). Two- to three-month-old male Copenhagen rats (Harlan-Sprague Dawley, Indianapolis, IN) were subcutaneously injected using a 26 gauge needle in the right flank with 1 x 10^6 cells suspended in 0.5 ml of Hanks Balanced Salt Solution (HBSS). Rats were allowed *ad libitum* access to water and standard rodent chow. All experimental procedures in this study received approval from the Institutional Laboratory Animal Care and Use Committee of The Ohio State University. Tumor size at the site of injection was measured with microcalipers weekly and at necropsy, and tumor volumes were calculated in cubic centimeters using the equation: volume = length x width x height x 0.5236 (17).

Tumorigenicity in Nude Mice

One million cells were resuspended in 200 μl of phosphate buffered saline and subcutaneously injected using a 26 gauge needle in the left (parental MATLyLu cells, n=6; MATLyLu-LXSN-mixed, n=6) and right (MATLyLu-FLhNIS-mixed, n=12) flanks of BALB/c athymic nude mice (male, 6-8 weeks-old; Harlan Sprague Dawley). Mice were maintained under pathogen-free conditions and allowed *ad libitum* access to water and standard rodent chow. Tumor size at the site of injection was measured with microcalipers three times a week and at necropsy, and tumor volumes were calculated in cubic millimeters as described above.

Histopathology

Complete postmortem and histopathological evaluations were performed on all rodents. Portions of the subcutaneous tumors, lymph node metastases, and lungs were fixed in 10% neutral-buffered formalin, routinely processed and embedded in paraffin. Sections (5 μm) were stained with hematoxylin and eosin (HE).

Immunohistochemistry

Immunohistochemical staining was performed on 5 μm paraffin sections cut onto poly-L-lysine slides. Sodium/iodide symporter immunohistochemistry was performed as previously described with a few modifications (18). Briefly, slides were incubated for 30 min in 10 mM citric acid buffer (pH 6.0) at 94C for antigen retrieval. Endogenous peroxidase was inhibited by 3% hydrogen peroxide in methanol. Tissue sections were incubated with an anti-hNIS proprietary polyclonal rabbit antibody (#331; 1:250 dilution) at room temperature for 1 hr, followed by avidin and biotin block (DAKO Corporation, Carpinteria, CA) for 10 min each, and then incubation with biotinylated goat anti-rabbit IgG (Bio-Rad Laboratories, Hercules, CA) for 20 min. Proliferation was assessed by Ki-67 immunostaining. Antigen retrieval was performed in 1X Reveal solution (Biocare Medical, Walnut Creek, CA) and endogenous peroxidase was inhibited by 3% hydrogen peroxide in distilled water. Tissue sections were incubated with an anti-rat Ki-67 mouse monoclonal antibody (clone MIB-5; 1:25 dilution, DAKO) at room temperature for 1 hr, followed by incubation with rat absorbed goat anti-mouse

IgG (Biocare Medical) for 30 minutes. Apoptosis was evaluated by caspase-3 immunostaining. Antigen retrieval was performed in 1X Reveal solution and endogenous peroxidase was inhibited by 3% hydrogen peroxide in distilled water. Tissue sections were incubated at room temperature for 1 hr with a polyclonal antibody (1:100 dilution, Cell Signaling, Beverly, MA) that specifically recognizes the large fragment of activated caspase-3. Specific binding for all stains was amplified using streptavidin horseradish-peroxidase. Chromogen reaction was developed with 3-3' diaminobenzidine (DAB) solution (DAKO), and nuclei were counterstained with hematoxylin.

Computer-Assisted Image Analysis

For each Ki-67 and caspase-3 stained slide, 2500 nuclei were randomly selected for analysis. For the purposes of this study, the labeling index (LI) for Ki-67 and caspase-3 was defined as: (number of Ki-67 or caspase-3 positive cells/total number of cells) x 100. Ki-67 and caspase-3 LIs were calculated as previously described (19). Briefly, histologic fields were captured with a charge-coupled device (CCD) Sony DKC ST5 camera (Sony, New York, NY) and digitized images were electronically recorded on a computer with a framegrabber board, providing permanent records of the exact specimens evaluated. Images were processed as necessary and then segmented using segmentation techniques such as density and size thresholding with or without dilation and erosion to distinguish negative from positive objects. The segmentation process results in the generation of binary images. The Optimas 6.5 image analysis

software (Optimas, Bothell, WA) generated the measurements of interest and the numerical data were statistically analyzed as described below.

In Vitro Growth Curve

Twelve-well plates were seeded with 1 x 10^3 parental or transduced MATLyLu cells per well. Each cell line was plated in triplicate. Cells were detached with 0.25% trypsin/EDTA and counted with a hemocytometer on days 1, 2, 4, 6 and 8.

In Vitro Electron Microscopy

Subconfluent parental or transduced MATLyLu cells were detached from T-75 flasks with 0.25% trypsin/EDTA, pelleted by centrifugation at 1000 rpm for 5 min at room temperature, and resuspended in 0.01% agarose dissolved in HBSS. Pellets were fixed in 3% glutaraldehyde, 1 M cacodylate buffer, and osmium tetroxide, and then embedded in medcast plastic (Ted Pella Redding, Redding, CA). Ultrathin sections were examined with a Philips 300 transmission electron microscope.

Statistical Analysis

Numerical data were expressed as means ± the standard error of the mean (SEM). Statistical differences between means for different data sets were evaluated with GraphPad Instat version 3.0 (GraphPad software, San Diego, CA)

using one-way analysis of variance (ANOVA) and Tukey-Kramer multiple comparisons test. Statistical significance was indicated by $P < 0.05$.

RESULTS

Decreased Growth and Slower Metastatic Progression of MATLyLu-hNIS Tumors in Copenhagen Rats

Six different *in vivo* experiments were conducted with MATLyLu cells from three different sources (Dr. Laurie McCauley, European Collection of Cell Culture [ECACC], Dr. Albert Geldof). Copenhagen rats were subcutaneously injected with either parental MATLyLu cells, MATLyLu cells transduced with vector only (LXSN) retrovirus, or MATLyLu cells transduced with retrovirus expressing the truncated form (hNIS#9) or the full-length form (FLhNIS) of hNIS. Rats were injected with a mixed population of MATLyLu-hNIS cells in four experiments whereas a clonal population was injected in two experiments. In all these experiments, NIS-transduced tumors were significantly smaller than control tumors regardless of the source of the MATLyLu cells, the hNIS construct used to make retrovirus, or whether the tumors were derived from mixed or clonal populations of transduced cells. The results are summarized in Table 1. Initially, rats were injected with either parental cells or a clonal population of MATLyLu-hNIS#9 cells. Although the sample size was small, the three MATLyLu-hNIS#9 tumors were 21-fold smaller than the parental MATLyLu tumor (McCauley, Table 1). Due to the inability to consistently produce lymph node and lung metastases

following subcutaneous injection of these parental MATLyLu cells, new MATLyLu cells were obtained from ECACC. In two subsequent *in vivo* experiments, rats were injected with parental MATLyLu cells or a mixed population of MATLyLu-FLhNIS cells. MATLyLu-FLhNIS tumors were 5- to 10-fold smaller than parental tumors in these experiments (ECACC, Table 1). However, the ECACC cells also failed to consistently metastasize following subcutaneous injection. In contrast, lymph node and lung metastases consistently developed when MATLyLu cells obtained from Dr. Geldof were subcutaneously injected in Copenhagen rats, and these cells were used in all subsequent experiments. These MATLyLu cells were transduced with retrovirus expressing LXSN or FLhNIS, and rats were injected with either mixed or clonal populations of transduced cells. MATLyLu-FLhNIS tumors were significantly smaller than control MATLyLu-LXSN tumors (Geldof, Table 1). The differences in tumor size were much more evident when a clonal population (18-fold smaller) of MATLyLu-FLhNIS cells was injected in the rats (Figure 1) compared to a mixed population (2- to 5-fold smaller).

Transduced MATLyLu cells from Dr. Geldof metastasized just as consistently as the parental cells with regard to frequency and site; however, the metastatic rate was delayed for LXSN-transduced tumors and even slower for NIS-transduced tumors. Following injection of parental cells, a prominent subcutaneous tumor was palpable by 7 days post-injection (dpi); however, LXSN- and NIS-transduced tumors were barely palpable at this time. Normally, ipsilateral axillary lymph nodes are not palpable in rats. Lymph nodes containing metastatic parental MATLyLu cells (confirmed by histology) were palpable 17 dpi

while LXSN or FLhNIS lymph node metastases were not palpable until 21 dpi. Furthermore, rats bearing parental MATLyLu tumors exhibited dyspnea indicative of diffuse pulmonary metastases (confirmed at necropsy) necessitating euthanasia at 24 dpi. In rats bearing MATLyLu-LXSN or MATLyLu-FLhNIS tumors, pulmonary metastases and extensive subcutaneous tumor burden necessitated euthanasia beyond 24 dpi. Rats with mixed LXSN tumors were sacrificed by 32 dpi and those with mixed FLhNIS tumors by 38 dpi, while those with clonal LXSN and FLhNIS tumors were sacrificed by 37 and 46 dpi, respectively.

Delayed Growth *In Vitro* of Clonal FLhNIS Cells

Growth curves were generated by counting parental MATLyLu cells, as well as a mixed population and 2 different clones of MATLyLu-LXSN and MATLyLu-FLhNIS cells over 8 days to investigate the growth rate of parental and transduced MATLyLu cells *in vitro* (Figure 2). Cells had reached confluency and were detaching from the wells by 8 days post-seeding. By 6 days post-seeding, a significant difference ($P < 0.001$) in cell number was only apparent between the FLhNIS clones and the parental cells or the LXSN clones; however, there was no difference in the growth rate *in vitro* between the mixed transduced cells and the parental cells in contrast to what was seen *in vivo*.

Variability in the Sizes of MATLyLu-FLhNIS Tumors in Athymic Nude Mice

Xenografts derived from parental MATLyLu, MATLyLu-LXSN and MATLyLu-FLhNIS cells were established in athymic nude mice to investigate whether a T cell-mediated immunologic effect contributed to the difference in growth rates *in vivo* between NIS-transduced and control tumors. All nude mice injected with parental and transduced MATLyLu cells developed prominent, palpable tumors by 7 dpi, but the sizes of NIS-transduced tumors were not consistently smaller or larger than those of parental or vector control tumors (Table 2). Control tumors were larger than FLhNIS tumors in 6 mice, while FLhNIS tumors were larger than control tumors in 5 mice. In 1 mouse, control and FLhNIS tumor sizes were equivalent. Although no statistically significant differences between mixed FLhNIS and control (parental, $P = 0.5476$; mixed LXSN, $P = 0.6967$) tumors were found, tumor volumes were smaller for FLhNIS tumors than control tumors (Table 2).

Outgrowth of NIS-Negative Cells in Tumors Derived from a Mixed MATLyLu-FLhNIS Cell Population

The distribution of cells expressing hNIS in tumors derived from a mixed population of MATLyLu-FLhNIS cells in Copenhagen rats and nude mice was evaluated by immunohistochemistry. Interestingly, it was noted that the distribution of NIS-positive cells in the majority of tumors was characterized by a well-demarcated region of heterogeneously immunoreactive cells circumferentially surrounded by an expansile band of NIS-negative (unstained)

cells (Figure 3A). This suggests that cells lacking NIS expression exhibit a growth advantage. As previously reported for tumors that are derived from a mixed population of retrovirally transduced cells, large numbers of MATLyLu-FLhNIS cells with intensely positive membrane staining were interspersed with unstained cells in the NIS-positive areas (Figure 3B) (3,9).

Decreased Proliferation in hNIS-Positive Areas of Rat Tumors Derived from a Mixed MATLyLu-FLhNIS Cell Population

Proliferation and apoptosis were evaluated by immunostaining tumors derived from mixed populations of MATLyLu-FLhNIS cells in Copenhagen rats (experiment 3) and nude mice for Ki-67 and caspase-3, respectively. The labeling index (LI) for each was compared between hNIS-positive and hNIS-negative areas of the tumors. The Ki-67 LI was significantly lower in hNIS positive areas than hNIS negative areas of mixed rat tumors (positive: 31.25 ± 6.07%; negative: 43.75 ± 6.62%; $P < 0.05$; n=5). There were no significant differences in the caspase-3 LI between the two areas in rat tumors (positive: 7.37 ± 3.45%; negative: 13.37 ± 5.77; $P = 0.3638$; n=5), or in the LIs for Ki-67 (positive: 84.35 ± 5.47%; negative: 85.61 ± 5.78%); $P = 0.7693$; n=6) or caspase-3 (positive: 1.59 ± 0.86%; negative: 1.01 ± 0.27%; P = 0.5165; n=6) in nude mouse tumors.

No Effect on Differentiation of MATLyLu Cells by NIS

In order to investigate whether exogenous hNIS expression induces differentiation of the anaplastic MATLyLu cells, microscopic morphology of the tumor cells *in vitro* and *in vivo*, as well as ultrastructural morphology *in vitro* was evaluated. There were no differences in morphology by phase contrast microscopy, transmission electron microscopy, or light microscopy between parental, LXSN-transduced and hNIS-transduced MATLyLu cells. Representative cells are illustrated in Figure 4.

DISCUSSION

The results of this study clearly demonstrate that growth of MATLyLu cells expressing exogenous hNIS is decreased *in vitro* and *in vivo*. Subcutaneous tumors were smaller and metastatic progression was slower in Copenhagen rats injected with MATLyLu-hNIS cells. This effect on *in vivo* growth was consistently observed in six different experiments and occurred independent of the source of MATLyLu cells, the hNIS construct used to generate retrovirus, and whether the tumors were derived from mixed or clonal populations of transduced cells. MATLyLu-FLhNIS tumors in nude mice had a lower, albeit not statistically significant, growth rate than control tumors. Growth of the clonal populations of NIS-transduced cells was significantly decreased compared to parental or clonal LXSN-transduced cells *in vitro*. Furthermore, the pattern of hNIS immunohistochemical staining in Copenhagen rat and nude mouse tumors

derived from mixed populations of MATLyLu-FLhNIS cells demonstrated that NIS-positive cells were confined to a central defined region surrounded by a band of NIS-negative cells.

Although previous studies investigating the utility of NIS gene transfer to facilitate radioiodide therapy for various cancers have not reported overt differences in growth between NIS-positive and NIS-negative tumors, Haberkorn and Shimura reported reduced weights of hNIS- and rNIS-expressing tumors compared to parental tumors in syngeneic rats, suggesting a similar effect (5,7). In addition, axillary lymph node metastases were previously only detected by nuclear scintigraphy in 3/12 rats injected with a mixed population of MATLyLu-FLhNIS cells, and NIS expression was absent by immunohistochemistry in the remaining lymph nodes (9). Taken together, these data suggest that MATLyLu cells lacking hNIS expression within a mixed population exhibit a growth advantage over NIS-expressing cells.

Possible mechanisms contributing to this *in vivo* growth difference include a direct effect by NIS on cell growth by decreasing proliferation, increasing apoptosis, and/or inducing cell cycle arrest. A decrease in proliferation was supported by the immunohistochemical results for Ki-67 in mixed MATLyLu-FLhNIS rat tumors, in which the Ki-67 LI was decreased in NIS-positive areas compared to the surrounding NIS-negative areas. Increased apoptosis was not evident by caspase-3 immunostaining, and pyknotic nuclei/apoptotic bodies were not apparent on histologic evaluation of MATLyLu-hNIS tumors. In addition to inducing apoptosis through a p53-independent mechanism (20,21), excess

iodide has been shown to inhibit growth of FRTL-5 rat thyroid cells through cell cycle arrest (22-24).

NIS is a marker of differentiation in the thyroid gland (1,25,26). This is evidenced by the fact that avidity for radioiodide is positively correlated with NIS expression and differentiation in thyroid cancer (27-29). The presence of NIS in transduced MATLyLu tumors may be causing the anaplastic MATLyLu cells to become more differentiated. However, the histological and ultrastructural morphology of MATLyLu-FLhNIS cells *in vitro* and *in vivo* was indistinguishable from that of MATLyLu-LXSN or parental cells. Tumors were equally anaplastic with numerous mitotic figures and comparable regions of necrosis. Subcutaneous MATLyLu-FLhNIS tumors also metastasized with the same frequency and to identical sites (ipsilateral regional lymph nodes, axillary lymph node, and lungs) as control tumors, just at later times. It is also unlikely that the constitutive transport of two Na^+ ions with one I^- ion has any adverse effect on cellular homeostasis since the sodium gradient is maintained by a Na^+/K^+ pump (1).

The fact that MATLyLu-hNIS tumors were consistently smaller than control tumors in immunocompetent syngeneic rats but were not always smaller than control tumors in immunodeficient mice suggests that an immunologic effect may also be contributing to the decreased growth of MATLyLu-hNIS tumors *in vivo*. Possible sources of immunogenicity in this study include the xenogeneic cell lines, the retroviral vector, in particular the neomycin resistance gene, and hNIS. NIS is an endogenous gene present in numerous tissues in addition to the

thyroid gland such as salivary glands, gastric mucosa, lactating mammary gland, kidney, and placenta (30-36). Although human NIS shares 84% identity with rat and mouse NIS (37,38), it has been identified as an autoantigen in patients with autoimmune thyroid disease (39,40). Despite this, growth of MATLyLu-hNIS tumors in Copenhagen rats and nude mice was not associated with an inflammatory cell response at either the primary or metastatic sites. However, this does not exclude the role of a humoral response. These animals have extensive tumor burdens, and numerous cytokines are likely to be elevated.

A final mechanism that must be considered is the effect of retroviral integration on the growth rate differences. Retroviral vectors are attractive methods of gene delivery because they stably integrate into the chromosome providing for long-term expression (12,41). The process of integration, which is random, involves a prefatory cleavage reaction and a subsequent strand-transfer reaction (42). Depending on the site of integration of retrovirus expressing hNIS, various *cis*-acting elements may be modulating the expression of hNIS. Such an explanation would be likely if the growth rate differences *in vivo* were only apparent with a clonal population of hNIS-transduced cells, as was observed *in vitro*. However, the differences in growth were also consistently seen in 4 different *in vivo* experiments using a mixed population of hNIS-transduced cells.

This study indicates that exogenous NIS expression causes decreased growth of subcutaneous MATLyLu tumors and slower metastatic progression, although the exact mechanism for this effect remains to be elucidated. Investigators need to be aware of these growth rate differences between tumors

with and without hNIS expression in the absence of radioiodide treatment. Such growth rate differences make interpretation of tumor regression, metastatic progression, and animal survival after radioiodide therapy difficult, and emphasize the need for the inclusion of appropriate treatment and vector controls. This decreased growth could provide an additional potential benefit of NIS-mediated gene therapy for the treatment of cancer.

ACKNOWLEDGEMENTS

We thank Dr. Albert Geldof and Dr. Laurie McCauley for the MATLyLu cells; Dr. Kathleen Boris-Lawrie for the LXSN retroviral vector; Ms. Anjli Venkateswaran, Ms. Danielle Westfall, and Mr. Marc Lavender for assistance with animal injections and postmortem evaluations; Dr. Richard Kloos for scientific discussion; Ms. Kathy Hopwood for animal husbandry; Mr. Alan Flechtner and Ms. Anne Saulsbery for histology slide preparation; Ms. Evelyn Handley and Ms. Mary Gessford for electron microscopy and immunohistochemistry support, respectively; and, Ms. Heather Caprette and Mr. Marc Hardman for assistance with photography and figure illustrations.

Address reprint requests to: Sissy M. Jhiang, The Ohio State University, Department of Physiology and Cell Biology, 304 Hamilton Hall, 1645 Neil Avenue, Columbus, OH 43210, Phone: 614-292-4312, Fax: 614-292-4888, Email: Jhiang.1@osu.edu.

REFERENCES

1. Carrasco N 1993 Iodide transport in the thyroid gland. Biochim Biophys Acta **1154**:65-82.

2. Mazzaferri EL 2000 Carcinoma of follicular epithelium: Radioiodine and other treatments and outcomes. In: Braverman LE, Utiger RD (ed) Werner and Ingbar's The Thyroid: A Fundamental and Clinical Text. Lippincott Williams and Wilkins, Philadelphia, pp. 904-929.

3. Boland A, Ricard M, Opolon P, Bidart J-M, Yeh P, Filetti S, Schlumberger M, Perricaudet M 2000 Adenovirus-mediated transfer of the thyroid sodium/iodide symporter gene into tumors for a targeted radiotherapy. Cancer Res **60**:3484-3492.

4. Nakamoto Y, Saga T, Misaki T, Kobayshi H, Sato N, Ishimori T, Kosugi S, Sakahara H, Konishi J 2000 Establishment and characterization of a breast cancer cell line expressing Na+/I- symporters for radioiodide concentrator gene therapy. J Nucl Med **41**:1898-1904.

5. Haberkorn U, Henze M, Altmann A, Jiang S, Morr I, Mahmut M, Peschke P, Kübler W, Debus J, Eisenhut M. Transfer of the human NaI symporter gene enhances iodide uptake in hepatoma cells. J Nucl Med **42**:317-325.

6. Mandell RB, Mandell LZ, Link CJ, Jr 1999 Radioisotope concentrator gene therapy using the sodium/iodide symporter gene. Cancer Res **59:**661-668.

7. Shimura H, Haraguchi K, Miyazaki A, Endo T, Onaya T 1997 Iodide uptake and experimental 131I therapy in transplanted undifferentiated thyroid cancer cells expressing the Na+/I- symporter gene. Endocrinology **138:**4493-4496.

8. Smit JW, Schröder-van der Elst JP, Karperien M, Que I, Stokkel M, van der Heide D, Romijn JA 2002 Iodide kinetics and experimental (131)I therapy in a xenotransplanted human sodium-iodide symporter-transfected human follicular thyroid carcinoma cell line. J Clin Endocrinol Metab **87:**1247-1253.

9. La Perle KMD, Shen D, Buckwalter TLF, Williams B, Haynam A, Hinkle G, Pozderac G, Capen CC, Jhiang SM 2002 In vivo expression and function of the sodium iodide symporter following gene transfer in the MATLyLu rat model of metastatic prostate cancer. Prostate **50:**170-178.

10. Spitzweg C, O'Connor MK, Bergert ER, Tindall DJ, Young CY, Morris JC 2000 Treatment of prostate cancer by radioiodine therapy after tissue-specific expression of the sodium iodide symporter. Cancer Res **60:**6526-6530.

11. Spitzweg C, Dietz AB, O'Connor MK, Bergert ER, Tindall DJ, Young CYF, Morris JC 2001 In vivo sodium iodide symporter gene therapy of prostate cancer. Gene Ther **8:**1524-1531.

12. Miller A, Rosman G 1989 Improved retroviral vectors for gene transfer and expression. Biotechniques **7:**980-990.

13. Dunning W 1963 Prostate cancer in the aging rat. Monogr Natl Cancer Inst **12:**351-369.

14. Isaacs JT, Yu GW, Coffey DS 1981 The characterization of a newly identified, highly metastatic variety of Dunning R 3327 rat prostatic adenocarcinoma system: The MAT LyLu tumor. Invest Urol **19:**20-23.

15. Geldof AA, Rao BR 1990 Factors in prostate cancer metastasis. Anticancer Res **10:**1303-1306.

16. Vieweg J, Heston WD, Gilboa E, Fair WR 1994 An experimental model simulating local recurrence and pelvic lymph node metastasis following orthotopic induction of prostate cancer. Prostate **24:**291-298.

17. Janik P, Briand P, Hartmann NR 1975 The effect of estrone-progesterone treatment on cell proliferation kinetics of hormone-dependent GR mouse mammary tumors. Cancer Res **35:**3698-3704.

18. Jhiang SM, Cho JY, Ryu KY, DeYoung BR, Smanik PA, McGaughy VR, Fischer AH, Mazzaferri EL 1998 An immunohistochemical study of Na+/I- symporter in human thyroid tissues and salivary gland tissues. Endocrinology **139:**4416-4419.

19. Baron DA, La Perle KMD, Blomme EAG 2000 The use of computer-assisted image analysis in the evaluation of preclinical tumor efficacy models. Curr Opin Drug Disc Devel **3:**79-93.

20. Burikhanov RB, Matsuzaki S 2000 Excess iodine induces apoptosis in the thyroid of goitrogen-pretreated rats in vivo. Thyroid **10:**123-129.

21. Vitale M, Di Matola T, D'Ascoli F, Salzano S, Bogazzi F, Fenzi G, Martino E, Rossi G 2000 Iodide excess induces apoptosis in thyroid cells through a p53-independent mechanism involving oxidative stress. Endocrinology **141**:598-605.

22. Saji M, Isozaki O, Tsushima T, Arai M, Miyakawa M, Ohba Y, Tsuchiya Y, Sano T, Shizume K. The inhibitory effect of iodide on growth of rat thyroid (FRTL-5) cells. Acta Endocrinol (Copenh) **119**:145-151.

23. Becks GP, Eggo MC, Burrow GN 1988 Organic iodine inhibits deoxyribonucleic acid synthesis and growth in FRTL-5 thyroid cells. Endocrinology **123**:545-551.

24. Smerdely P, Pitsiavas V, Boyages SC 1993 Evidence that the inhibitory effects of iodide on thyroid cell proliferation are due to arrest of the cell cycle at G0G1 and G2M phases. Endocrinology **133**:2881-2888.

25. Damante G, Di Lauro R 1994 Thyroid-specific gene expression. Biochim Biophys Acta **1218**:255-266.

26. Lazar V, Bidart JM, Caillou B, Mahe C, Lacroix L, Filetti S, Schlumberger M 1999 Expression of the Na+/I- symporter gene in human thyroid tumors: A comparison study with other thyroid-specific genes. J Clin Endocrinol Metab **84:**3228-3234.

27. Caillou B, Troalen F, Baudin E, Talbot M, Filetti S, Schlumberger M, Bidart JM 1998 Na+/I- symporter distribution in human thyroid tissues: An immunohistochemical study. J Clin Endocrinol Metab **83:**4102-4106.

28. Min JJ, Chung JK, Lee YJ, Jeong JM, Lee DS, Jang JJ, Lee MC, Cho BY 2001 Relationship between expression of the sodium/iodide symporter and 131I uptake in recurrent lesions of differentiated thyroid carcinoma. Eur J Nucl Med **28:**639-645.

29. Castro MR, Bergert ER, Goellner JR, Hay ID, Morris JC 2001 Immunohistochemical analysis of sodium iodide symporter expression in metastatic differentiated thyroid cancer: Correlation with radioiodine uptake. J Clin Endocrinol Metab **86:**5627-5632.

30. Spitzweg C, Joba W, Eisenmenger W, Heufelder AE 1998 Analysis of human sodium iodide symporter gene expression in extrathyroidal tissues and cloning of its complementary deoxyribonucleic acids from salivary gland, mammary gland, and gastric mucosa. J Clin Endocrinol Metab **83:**1746-1751.

31. Jhiang SM. Regulation of sodium/iodide symporter. Rev Endocr Metab Disord **1:**205-215.

32. Perron B, Rodriguez AM, Leblanc G, Pourcher T 2001 Cloning of the mouse sodium iodide symporter and its expression in the mammary gland and other tissues. J Endocrinol **170:**185-196.

33. Tazebay UH, Wapnir IL, Levy O, Dohan O, Zuckier LS, Zhao QH, Deng HF, Amenta PS, Fineberg S, Pestell RG, Carrasco N 2000 The mammary gland iodide transporter is expressed during lactation and in breast cancer. Nat Med **6:**871-878.

34. Kotani T, Ogata Y, Yamamoto I, Aratake Y, Kawano JI, Suganuma T, Ohtaki S 1998 Characterization of gastric Na+/I- symporter of the rat. Clin Immunol Immunopathol **89:**271-278.

35. Mitchell AM, Manley SW, Morris JC, Powell KA, Bergert ER, Mortimer RH 2001 Sodium iodide symporter (NIS) gene expression in human placenta. Placenta **22:**256-258.

36. Spitzweg C, Dutton CM, Castro MR, Bergert ER, Goellner JR, Heufelder AE, Morris JC 2001 Expression of the sodium iodide symporter in human kidney. Kidney Int **59:**1013-1023.

37. Smanik PA, Liu Q, Furminger TL, Ryu K, Xing S, Mazzaferri EL, Jhiang SM 1996 Cloning of the human sodium iodide symporter. Biochem Biophys Res Commun **226:**339-345.

38. Pinke LA, Dean DS, Bergert ER, Spitzweg C, Dutton CM, Morris JC 2001 Cloning of the mouse sodium iodide symporter. Thyroid **11:**935-939.

39. Endo T, Kogai T, Nakazato M, Saito T, Kaneshige M, Onaya T 1996 Autoantibody against Na+/I- symporter in the sera of patients with autoimmune thyroid disease. Biochem Biophys Res Comm **224:**92-95.

40. Endo T, Kaneshige M, Nakazato M, Kogai T, Saito T, Onaya T 1996 Autoantibody against thyroid iodide transporter in the sera from patients with Hashimoto's thyroiditis possesses iodide transport inhibitory activity. Biochem Biophys Res Comm **228:**199-202.

41. Anderson WF 1998 Human gene therapy. Nature **392**:25-30.

42. Hindmarsh P, Leis J 1999 Retroviral DNA integration. Microbiol Mol Biol Rev **63**:836-843.

FIGURE LEGENDS

Figure 1: Appearance of subcutaneous tumors (indicated by arrows) in Copenhagen rats 22 days following injection of a clonal population of MATLyLu-FLhNIS cells (A) and MATLyLu-LXSN cells (B). The MATLyLu-FLhNIS tumor is significantly smaller than the MATLyLu-LXSN tumor.

Figure 2: Growth of parental (solid line) and transduced MATLyLu cells *in vitro*. A mixed population (M) and 2 different individual clones (1, 2) were evaluated for MATLyLu cells transduced with empty vector (LXSN, dotted lines) retrovirus or retrovirus expressing FLhNIS (NIS, dashed lines). Six days post-seeding, a significant difference ($P < 0.001$) in cell number was only apparent between the FLhNIS clones and the parental cells or the LXSN clones. There was no difference *in vitro* between the mixed transduced cells and the parental cells as seen *in vivo*.

Figure 3: Immunohistochemical stain for hNIS in a subcutaneous MATLyLu-FLhNIS tumor from an athymic nude mouse. The distribution of NIS-positive cells is characterized by a well-demarcated central region of heterogeneously immunoreactive cells (A) circumferentially surrounded by an expansile band of NIS-negative (unstained) cells (x20). The border (B) between NIS-positive and NIS-negative cells is distinct. Within the NIS-positive areas, large numbers of MATLyLu-FLhNIS cells with intensely positive membrane staining are

interspersed with unstained cells, a staining pattern consistent for tumors that are derived from a mixed population of retrovirally-transduced cells (avidin-biotin complex immunoperoxidase method, hematoxylin counterstain, x200).

Figure 4: Morphological appearance of MATLyLu-FLhNIS cells by phase contrast microscopy (A), transmission electron microscopy (B), and light microscopy (C). The morphology of parental and MATLyLu-LXSN cells was similar. Ultrastructurally (B), an irregularly round nucleus with a heterochromatic nucleolus, as well as mitochondria (arrow) and rare lysosomes (*) in the cytoplasm are apparent (Uranyl acetate and lead citrate, x4859). Histologically (C), tumor cells are anaplastic with numerous atypical mitotic figures (Hematoxylin and eosin, x400).

Table 1. hNIS-Transduced and Control Subcutaneous MATLyLu Tumor Volumes in Copenhagen Rats

Experiment	Tumor Type	Cell Source	Clonality	Tumor Volume (cm^3) Mean ± SEM[a]	Days Post-Injection	Sample Size	*P* Value
1	Parental	McCauley	N/A	15.46 ± 0.0	21	1	N/A
1	hNIS#9	McCauley	Clonal	0.74 ± 0.18	21	3	N/A[b]
2	Parental	ECACC	N/A	1.05 ± 0.21	11	4	N/A
2	FLhNIS	ECACC	Mixed	0.23 ± 0.09	11	4	< 0.05
3	Parental	ECACC	N/A	2.20 ± 0.44	10	2	N/A
3	FLhNIS	ECACC	Mixed	0.22 ± 0.03	10	4	< 0.001
4	LXSN	Geldof	Mixed	16.25 ± 1.03	21	7	N/A
4	FLhNIS	Geldof	Mixed	7.60 ± 1.32	21	8	< 0.001
5	LXSN	Geldof	Mixed	10.60 ± 1.28	18	4	N/A
5	FLhNIS	Geldof	Mixed	2.25 ± 0.73	18	6	< 0.01
6	LXSN	Geldof	Clonal	12.77± 1.21	22	10	N/A
6	FLhNIS	Geldof	Clonal	0.71 ± 0.15	22	16	< 0.001

[a]SEM: Standard error of the mean

[b]Sample size too small for statistical analysis

Table 2. FLhNIS-Transduced and Control MATLyLu Subcutaneous Tumor Volumes in Athymic Nude Mice

[a]Parental MATLyLu	MATLyLu-FLhNIS-Mixed
498.47 mm^3	54.98 mm^3
130.90 mm^3	50.27 mm^3
69.12 mm^3	69.12 mm^3
141.37 mm^3	219.90 mm^3
197.92 mm^3	502.66 mm^3
230.91 mm^3	4.19 mm^3
Mean ± SEM[b]: 211.45 ± 61.81 mm^3	Mean ± SEM: 50.19 ± 76.60 mm^3

[c]Mixed MATLyLu-LXSN	Mixed MATLyLu-FLhNIS
104.72 mm^3	150.90 mm^3
26.18 mm^3	628.32 mm^3
570.20 mm^3	47.12 mm^3
628.32 mm^3	37.70 mm^3
263.89 mm^3	134.04 mm^3
131.95 mm^3	153.94 mm^3
Mean ± SEM: 287.54 ± 103.69 mm^3	Mean ± SEM: 191.99 ± 89.76 mm^3

[a]One group of mice (n=6) subcutaneously injected in the left flank with parental MATLyLu cells and in the right flank with a mixed population of MATLyLu-FLhNIS cells

[b]SEM: Standard error of the mean

[c]Second group of mice (n=6) subcutaneously injected in the left flank with a mixed population of MATLyLu-LXSN cells and in the right flank with a mixed population of MATLyLu-FLhNIS cells

Figure 1.

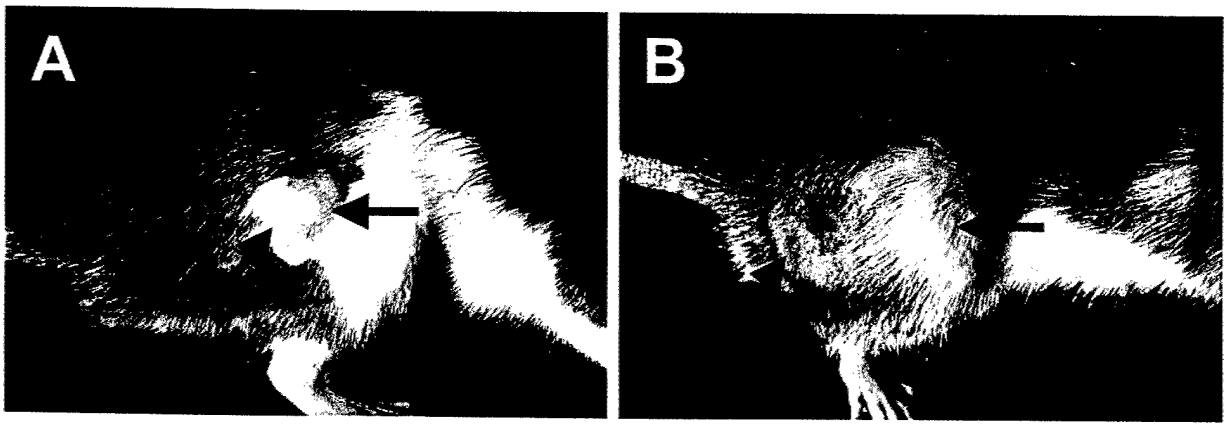

Figure 2.

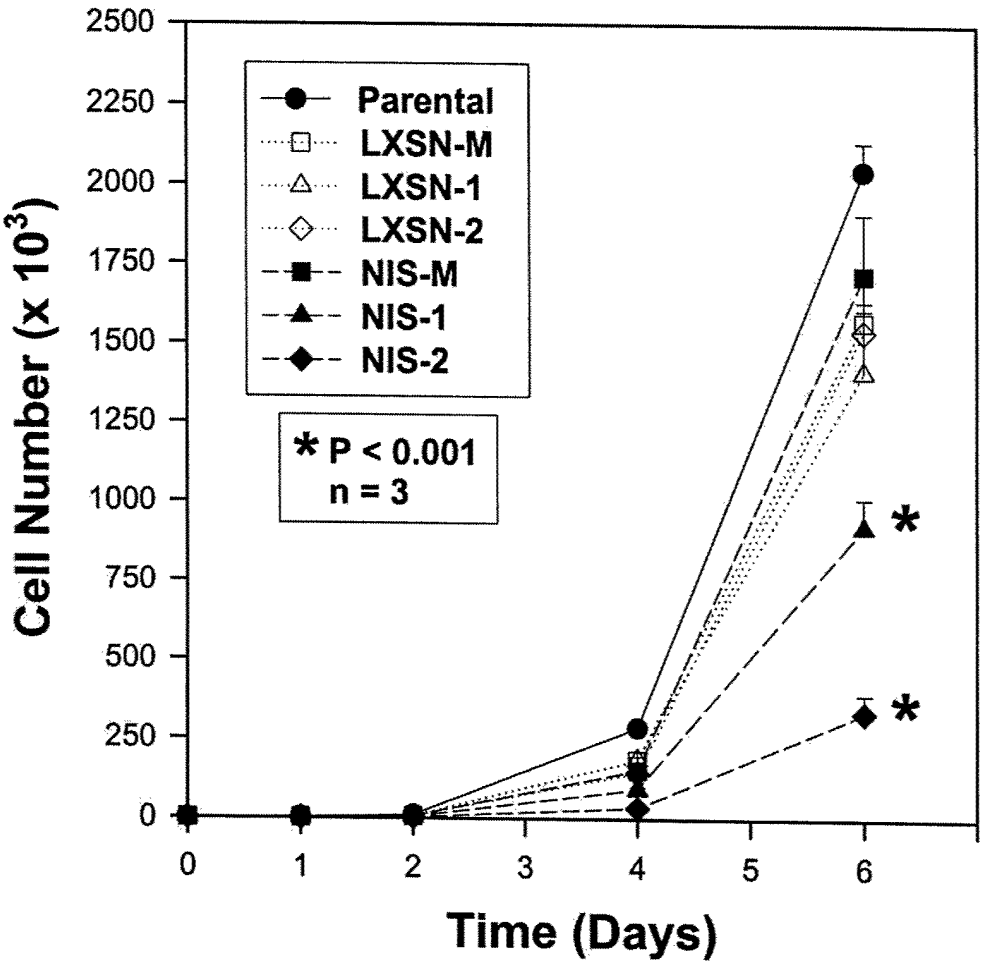
Cell Number (x 10^3)
2500
2250
2000
1750
1500
1250
1000
750
500
250
0
0
1
2
3
4
5
6
Time (Days)
Parental
LXSN-M
LXSN-1
LXSN-2
NIS-M
NIS-1
NIS-2
* P < 0.001
n = 3
*
*

Figure 3.

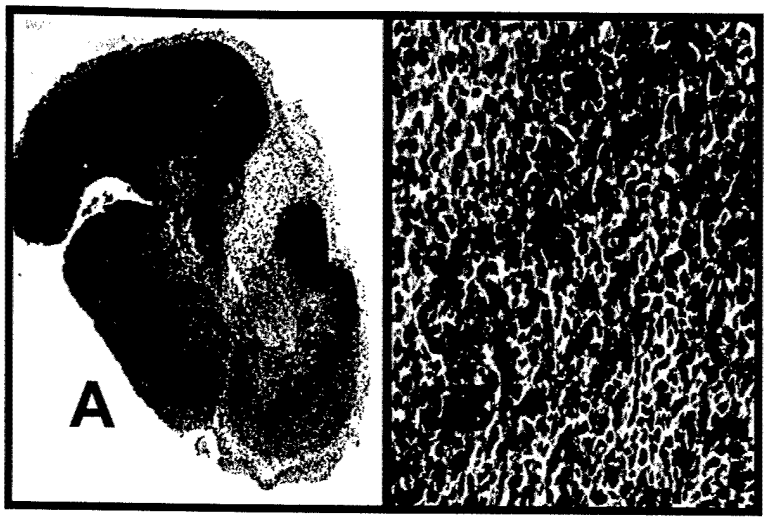

Figure 4.